

Anomalous absorption in thioformaldehyde

Suresh Chandra, Amit Kumar and M.K. Sharma

School of Physical Sciences, S.R.T.M. University, Nanded 431 606, India¹

Email: suresh492000@yahoo.co.in

Abstract. Absorption against the Cosmic Microwave Background (CMB), called the anomalous absorption, is an unusual phenomenon. The transition $1_{11} - 1_{10}$ at 4.829 GHz of formaldehyde (H_2CO) was the first one showing the anomalous absorption. The $c\text{-C}_3\text{H}_2$ is the second molecule showing anomalous absorption through its transition $2_{20} - 2_{11}$ at 21.590 GHz. Structure of thioformaldehyde (H_2CS) is very similar to that of the H_2CO . Therefore, we have investigated about the physical conditions under which the transition $1_{11} - 1_{10}$ at 1.0465 GHz of H_2CS would be found in anomalous absorption in cool cosmic objects. As in case of H_2CO , the anomalous absorption of $1_{11} - 1_{10}$ of H_2CS is found sensitive to the relative collisional rates and it requires that the collisional rate for the transition $1_{11} - 2_{11}$ must be smaller than that for the transition $1_{10} - 2_{12}$.

Key words. ISM: molecules

1 Introduction

Snyder et al. (1969) detected H_2CO through its transition $1_{10} - 1_{11}$ at 4.829 GHz in absorption in a number of galactic and extragalactic sources. This transition of H_2CO was found in anomalous absorption by Palmer et al. (1969) in the direction of four dark nebulae. In some objects, this transition has however been detected in emission and even as a maser line (Forster et al., 1980; Whiteoak et al., 1983). Observation of an interstellar line in absorption against the cosmic microwave background (CMB) is an unusual phenomenon. The second line found in absorption against the CMB, in a large number of cosmic objects, is the $2_{20} - 2_{11}$ transition of the cyclopropenylidene ($c\text{-C}_3\text{H}_2$) at 21.590 GHz (Madden et al., 1989). Cox et al. (1987), however, reported the observation of this line in emission in the Planetary Nebula NGC 7027.

Structure of thioformaldehyde (H_2CS) is very similar to that of the H_2CO (Figure 1). Keeping in view the similarity of H_2CO and H_2CS , in the present investigation, we attempted to look into the physical conditions under which the transition $1_{11} - 1_{10}$ at 1.0465 GHz of H_2CS may be found in anomalous absorption.

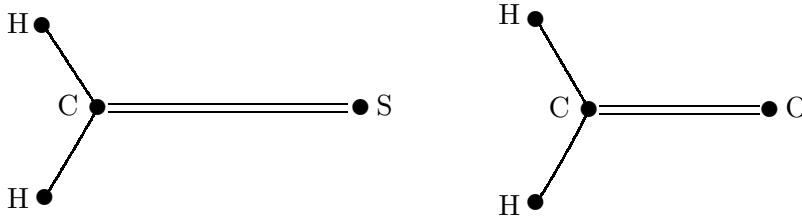


Figure 1: Structures of H_2CS and H_2CO molecules are very similar to each other.

¹Present address: School of Physics, Shri Mata Vaishno Devi University, Katra 182 320 (J&K), India

2 Thioformaldehyde

Thioformaldehyde is an *a*-type asymmetric top molecule having electric dipole moment 1.6491(4) Debye (Fabricant, 1977). The first microwave spectrum of thioformaldehyde (H₂CS) was studied by Johnson & Powell (1970). Following that the interstellar search for the transition 1₁₀ – 1₁₁ of H₂CS was carried out by Evans et al. (1970) and Davies et al. (1971), which remained unsuccessful. Johnson et al. (1971) and Beers et al. (1972) recorded improved rotational spectra and predicted a large number of lines to be identified in the interstellar medium. The first success for identification of H₂CS was reported by Sinclair et al. (1973) through the transition 2₁₁ – 2₁₂ at 3.139 GHz in Sgr B2 in absorption. The said predictions have been useful in the astronomical observations and eight lines of normal thioformaldehyde were found in the astronomical survey performed by Schilke et al. (1997) towards Orion KL, in the range from 325 to 365 GHz. The singly and doubly deuterated species of thioformaldehyde, HDCS and D₂CS, have been observed by Marcelino et al. (2005) toward the dark cloud Barnard 1.

Recently Maeda et al. (2008) studied pure rotational spectrum of H₂CS and derived very accurate molecular and distortional constants given in Table 1 where the observed frequencies were fitted to Watson’s *S*-reduction Hamiltonian using *I*^{*r*} representation (Gordy & Cook, 1984).

Table 1. Parameters of H₂CS and H₂CO in MHz

Parameter	H ₂ CS ^{<i>a</i>}	H ₂ CO ^{<i>b</i>}
A	$2.916133419858 \times 10^5$	$2.81970554688 \times 10^5$
B	$1.76989948807 \times 10^4$	$3.88339890137 \times 10^4$
C	$1.66524986641 \times 10^4$	$3.40042453613 \times 10^4$
<i>D_J</i>	$19.0210847 \times 10^{-3}$	$70.3210068 \times 10^{-3}$
<i>D_{JK}</i>	$522.283353 \times 10^{-3}$	$1321.10115 \times 10^{-3}$
<i>D_K</i>	23.344325	19.3908972
<i>d</i> ₁	$-1.2084913 \times 10^{-3}$	$-10.4379818 \times 10^{-3}$
<i>d</i> ₂	$-0.17734329 \times 10^{-3}$	$-2.50146158 \times 10^{-3}$
<i>H_J</i>	-3.3329×10^{-9}	3.9247×10^{-9}
<i>H_{JK}</i>	1.487734×10^{-6}	7.45331×10^{-6}
<i>H_{KJ}</i>	$-28.222103 \times 10^{-6}$	10.7216×10^{-6}
<i>H_K</i>	5.95849×10^{-3}	4.02125×10^{-3}
<i>h</i> ₁	3.085179×10^{-9}	3.23314×10^{-9}
<i>h</i> ₂	1.65623×10^{-9}	4.78713×10^{-9}
<i>h</i> ₃	0.32731×10^{-9}	1.594631×10^{-9}
<i>L_{JJK}</i>	-	-94.21×10^{-12}
<i>L_{JK}</i>	0.19622×10^{-9}	0.3310×10^{-9}
<i>L_{KKJ}</i>	-20.7881×10^{-9}	-4.5282×10^{-9}
<i>L_K</i>	-2.1726×10^{-6}	-0.5919×10^{-6}
<i>l</i> ₁	-0.37662×10^{-12}	-
<i>l</i> ₂	-	-0.30793×10^{-12}
<i>l</i> ₃	-	-0.42735×10^{-12}
<i>l</i> ₄	-	$-0.137543 \times 10^{-12}$

^{*a*} Maeda et al. (2008)

^{*b*} Brünken et al. (2003); the signs of *L_{KKJ}* and *L_K* are corrected.

3 Energy levels and Einstein A -Coefficients

In the present investigation, we want to address the cool cosmic objects having kinetic temperature of few tens of Kelvin. Therefore, we are concerned with the rotational transitions in the ground vibrational and electronic states. Owing to the parallel and anti-parallel orientations of nuclear spins of two hydrogen atoms in the molecule, the molecule can have two species, known as the ortho ($I = 1$) and para ($I = 0$). These two species behave as if they are two distinct molecules and there are no transitions between them.

Rotational wavefunctions for an asymmetric top molecule can be expressed as linear combinations of symmetric top wavefunctions (Chandra et al., 1984 a, b)

$$A_{J\tau M}(\alpha, \beta, \gamma) = \sqrt{\frac{2J+1}{8\pi^2}} \sum_{K=-J}^J g_{\tau K}^J D_{MK}^J(\alpha, \beta, \gamma)$$

where α, β, γ are Euler angles specifying the orientation of the molecule, J the rotational quantum number, $g_{\tau K}^J$ the expansion coefficients, D_{MK}^J the Wigner D-functions and the pseudo quantum number τ is defined as

$$\tau = k_a - k_c$$

where k_a and k_c are the projections of J on the axis of symmetry in case of prolate and oblate symmetric tops, respectively. Rotational levels in an asymmetric top molecule are specified as J_{k_a, k_c} or J_τ . Since the electric dipole moment of H_2CS is along the a -axis of inertia, the radiative transitions are governed by the selection rules:

$$\begin{aligned} J : & \Delta J = 0, \pm 1 \\ k_a, k_c : & \text{even, odd} \longleftrightarrow \text{even, even} \\ & \text{odd, even} \longleftrightarrow \text{odd, odd.} \end{aligned}$$

In the I^r representation, Einstein A -coefficient for the transition $J_{\tau'} \rightarrow J_\tau$ is given by (Chandra et al., 2006b)

$$A(J_{\tau'} \rightarrow J_\tau) = \frac{64\pi^4 \nu^3 \mu^2 S}{3hc^3(2J'+1)}$$

where

$$S = (2J+1) \left[\sum_{K=-J}^J g_{\tau K}^J g_{\tau' K}^{J'} C_{JK10}^{J'K} \right]^2$$

is the line strength, μ the electric dipole moment of molecule along the a -axis of inertia and $C_{JK10}^{J'K}$ the Clebsch Gordon coefficient. Using the molecular and distortional constants of Maeda et al. (2008), we obtained rotational energy levels and the lowest 25 of them, accounted for in the present investigation, are given in Table 2. These levels are connected by 36 radiative transitions for which the Einstein A -coefficients and $\mu^2 S(2I+1)$ are given in Table 3. Einstein B -coefficients can be obtained by using the standard relations between A - and B -coefficients. Here, $I = 1$ for the nuclear spin of ortho specie. The value of $\mu^2 S(2I+1)$ for the transition $1_{10} - 1_{11}$ is twice of that for the transition $2_{11} - 2_{12}$ (through which the molecule was identified). Hence, the transition $1_{10} - 1_{11}$ has large probability for its detection.

Table 2. Energy of rotational levels in ortho-H₂CS

Level	E (MHz)	Level	E (MHz)	Level	E (MHz)
1 _{1,1}	308241.386	5 _{1,4}	2506196.454	9 _{1,8}	4013434.545
1 _{1,0}	309287.873	6 _{1,6}	2575207.221	10 _{1,10}	4013439.435
2 _{1,2}	375895.218	6 _{1,5}	2674103.455	10 _{1,9}	4330966.231
2 _{1,1}	379034.620	7 _{1,7}	2674103.461	11 _{1,11}	4356844.521
3 _{1,3}	477373.028	7 _{1,6}	2811472.915	11 _{1,10}	4356853.601
3 _{1,2}	483651.652	8 _{1,8}	2811472.952	3 _{3,1}	4456308.627
4 _{1,4}	612671.297	8 _{1,7}	2911795.644	3 _{3,0}	4734591.192
4 _{1,3}	623135.255	9 _{1,9}	2983184.083	4 _{3,2}	4734607.077
5 _{1,5}	781785.349				

Table 3. Einstein *A*-coefficients and $\mu^2 S(2I + 1)$ for transitions

Transition	<i>A</i> -coeff (s ⁻¹)	$3\mu^2 S$ (D ²)	Transition	<i>A</i> -coeff (s ⁻¹)	$3\mu^2 S$ (D ²)
1 _{1,0} → 1 _{1,1}	1.814E-11	12.20	2 _{1,2} → 1 _{1,1}	2.941E-06	12.20
2 _{1,1} → 1 _{1,0}	3.222E-06	12.20	2 _{1,1} → 2 _{1,2}	1.632E-10	6.80
3 _{1,3} → 2 _{1,2}	1.260E-05	21.80	3 _{3,1} → 2 _{1,2}	1.098E-07	0.00
3 _{1,2} → 2 _{1,1}	1.381E-05	21.80	3 _{3,0} → 2 _{1,1}	1.093E-07	0.00
3 _{1,2} → 3 _{1,3}	6.529E-10	4.80	3 _{3,0} → 3 _{1,3}	9.588E-08	0.00
4 _{1,4} → 3 _{1,3}	3.267E-05	30.60	4 _{3,2} → 3 _{1,3}	2.684E-07	0.00
4 _{3,2} → 3 _{3,1}	1.596E-05	14.30	4 _{1,3} → 3 _{1,2}	3.579E-05	30.60
4 _{1,3} → 4 _{1,4}	1.814E-09	3.70	5 _{1,5} → 4 _{1,4}	6.681E-05	39.20
5 _{1,4} → 4 _{1,3}	7.320E-05	39.20	5 _{1,4} → 5 _{1,5}	4.080E-09	3.00
6 _{1,6} → 5 _{1,5}	1.187E-04	47.60	6 _{1,5} → 5 _{1,4}	1.301E-04	47.60
6 _{1,5} → 6 _{1,6}	7.995E-09	2.50	7 _{1,7} → 6 _{1,6}	1.920E-04	55.90
7 _{1,6} → 6 _{1,5}	2.103E-04	55.90	7 _{1,6} → 7 _{1,7}	1.421E-08	2.20
8 _{1,8} → 7 _{1,7}	2.903E-04	64.30	8 _{1,7} → 7 _{1,6}	3.181E-04	64.30
8 _{1,7} → 8 _{1,8}	2.349E-08	1.90	9 _{1,9} → 8 _{1,8}	4.173E-04	72.50
9 _{1,8} → 8 _{1,7}	4.573E-04	72.50	9 _{1,8} → 9 _{1,9}	3.669E-08	1.70
10 _{1,10} → 9 _{1,9}	5.767E-04	80.80	10 _{1,9} → 9 _{1,8}	6.318E-04	80.80
10 _{1,9} → 10 _{1,10}	5.480E-08	1.60	11 _{1,11} → 10 _{1,10}	7.720E-04	89.00
11 _{1,10} → 10 _{1,9}	8.458E-04	89.00	11 _{1,10} → 11 _{1,11}	7.889E-08	1.40

4 Basic formulation

For the kinetic temperature of 10 – 40 K in the cosmic objects, it is sufficient to account for 25 rotational energy levels of ortho-H₂CS (Table 2). In our investigation, we solved a set of statistical equilibrium equations coupled with equations of radiative transfer, given as the following:

$$n_i \sum_{\substack{j=1 \\ j \neq i}}^{25} P_{ij} = \sum_{\substack{j=1 \\ j \neq i}}^{25} n_j P_{ji} \quad i = 1, 2, \dots, 25$$

where *n*'s are the population densities of levels and *P*'s are expressed as the following:

(i) For optically allowed transitions

$$P_{ij} = \begin{cases} (A_{ij} + B_{ij} I_{\nu,bg})\beta_{ij} + n_{H_2} C_{ij} & i > j \\ B_{ij} I_{\nu,bg}\beta_{ij} + n_{H_2} C_{ij} & i < j \end{cases}$$

(ii) For optically forbidden transitions

$$P_{ij} = n_{H_2} C_{ij}$$

where A 's and B 's are Einstein coefficients, related as

$$A_{ul} = \frac{2h\nu^3}{c^2} B_{ul} \quad B_{ul} = \frac{g_l}{g_u} B_{lu}$$

C 's the collisional rate coefficients, n_{H_2} the density of hydrogen molecules, and the escape probability β for the transition is

$$\beta_{lu} = \beta_{ul} = \frac{1 - \exp(-\tau_\nu)}{\tau_\nu}$$

for spherically symmetric geometry. Here optical thickness τ_ν is

$$\tau_\nu = \frac{hc}{4\pi(dv_r/dr)} [B_{lu}n_l - B_{ul}n_u]$$

where (dv_r/dr) is velocity-gradient in the region. By solving these equations, populations of the levels are calculated. The suffixes u and l stand for the upper and lower levels, respectively. Here, external radiation field, impinging on a volume element generating the lines, is the CMB only. This set of equations is solved through iterative procedure for the given values of n_{H_2} and $\gamma \equiv n_{\text{mol}}/(dv_r/dr)$, where n_{mol} is density of the molecule.

5 Collisional rates

In the present investigation, besides the radiative transition probabilities, the collisional rate coefficients are required as input parameters. Though the collisional transitions are not restricted through any selection rules, computation of them is a quite cumbersome task. The required collisional rates are not available in the literature. In absence of collisional rates, qualitative investigation can be carried out by choosing some scaling laws, which do not favour any anomalous behaviour from their own. In the present investigation, the rate coefficients for downward transitions $J'_{k'_a k'_c} \rightarrow J_{k_a k_c}$ at a kinetic temperature T_k are taken as (Chandra et al., 2007)

$$C(J'_{k'_a k'_c} \rightarrow J_{k_a k_c}) = 1 \times 10^{-11} (2J + 1) \sqrt{\frac{T_k}{30}} \quad (1)$$

This relation for collisional rate coefficients can be interpreted as the cross-section times the thermal velocity. These rates have no selectivity and do not support any anomalous behaviour from their own. For upward collisional rate coefficients, we accounted for the

fact that downward and upward collisional rate coefficients are related through the detailed equilibrium (Chandra & Kegel, 2000):

$$C(J_{k_a k_c} \rightarrow J'_{k'_a k'_c}) = C(J'_{k'_a k'_c} \rightarrow J_{k_a k_c}) \frac{2J' + 1}{2J + 1} \exp\left(-\frac{\Delta E}{kT_k}\right)$$

where k is Boltzmann constant and ΔE the energy difference between upper and lower energy levels.

6 Anomalous absorption

The intensity, I_ν , of a line generated in an interstellar cloud, with homogeneous excitation conditions, is given by

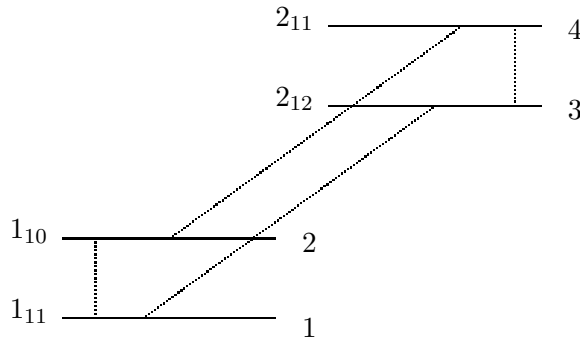
$$I_\nu - I_{\nu,bg} = (S_\nu - I_{\nu,bg})(1 - e^{-\tau_\nu})$$

where $I_{\nu,bg}$ is the intensity of continuum against which the line is observed, τ_ν the optical depth of the line and S_ν the source function. For positive optical depth, observation of an interstellar line in absorption against the CMB (*i.e.*, $I_\nu < I_{\nu,bg}$), obviously, implies the excitation temperature T_{ex} of the line to be less than the CMB-temperature T_{bg} , but positive ($0 < T_{ex} < T_{bg}$). It requires rather peculiar conditions in the molecule generating the line. In the Rayleigh-Jeans limit, we have

$$T_B = T_{ex} + (T_{bg} - T_{ex})e^{-\tau_\nu}$$

This obviously shows that for the optically thin case, $\tau_\nu \approx 0$ and we have $T_B = T_{bg}$. For anomalous absorption, the excitation temperature T_{ex} , brightness temperature T_B and the background temperature T_{bg} satisfy the condition $0 < T_{ex} < T_B < T_{bg}$. Here, the CMB temperature is 2.73 K.

Let us try to find out the requirement for the anomalous absorption for the transition $1_{11} - 1_{10}$. For this transition, the levels of the doublet $J = 1$ are radiatively connected to the levels of $J = 2$ doublet only, as shown in the following figure. For convenience, the levels are labeled as 1, 2, 3, 4. The radiatively allowed transitions between the levels are shown by the dotted lines.



In the optically thin limit ($n_{H_2}C_{ul} \ll A_{ul}$, *i.e.*, the collisional rates are negligible in comparison to the radiative ones), for these four energy levels, the statistical equilibrium

equations may be expressed as the following (Chandra et al., 2006a):

$$\begin{aligned}n_1(C_{13} + C_{14}) &= n_3A_{31} \\n_2(C_{23} + C_{24}) &= n_4A_{42} \\n_3A_{31} &= n_1C_{13} + n_2C_{23} \\n_4A_{42} &= n_1C_{14} + n_2C_{24}\end{aligned}$$

These equations can be rearranged as

$$\frac{n_2}{n_1} = \frac{C_{14}}{C_{23}}$$

For anomalous absorption, we require $n_2 < n_1$, showing that $C_{14} < C_{23}$. This shows that the transition between the levels 1_{11} and 1_{10} would show absorption against the CMB provided $C_{14} < C_{23}$. Since equation (1) gives $C_{14} = C_{23}$, we have to modify either C_{14} , C_{23} or both of them in order to get anomalous absorption.

7 Results and discussion

In our investigation, NLTE occupation numbers of levels are calculated in an on-the-spot approximation by using the method discussed in section 4, where the external radiation field, impinging on a volume element generating the lines, is the CMB only. In the present investigation, a set of 25 linear equations coupled with 36 equations of radiative transfer is solved through the iterative procedure for the given values of n_{H_2} and γ . In order to include a large number of cosmic objects where H_2CS may be found, numerical calculations are carried out for the wide ranges of physical parameters. In the present investigation, we have taken $\gamma = 10^{-6} \text{ cm}^{-3} (\text{km/s})^{-1} \text{ pc}$ and $10^{-5} \text{ cm}^{-3} (\text{km/s})^{-1} \text{ pc}$. For lower value of the column density, the intensity of the line may not be observable. The molecular hydrogen density n_{H_2} is varied over the range from 10^3 to 10^7 cm^{-3} , and calculations are made for the kinetic temperatures 10 K, 20 K, 30 K and 40 K, as the temperature in a cool cosmic object would be around that.

The collisional rates obtained from equation (1) give $C_{14} = C_{23}$. Hence, the required condition $C_{14} < C_{23}$ is not produced. This condition can be produced either by increasing the collision rates between the levels 1_{10} and 2_{12} by some positive factor greater than 1 or by reducing the collision rates between the levels 1_{11} and 2_{11} by a positive factor greater than 1 or by doing both.

(i) We increased the collisional rates for the transitions between the levels 1_{10} and 2_{12} by a factor of 2 and the result given in Figure 2 show the brightness temperature T_B (K) (column 1), excitation temperature T_{ex} (K) (column 2) and the optical depth τ_ν (column 3) as a function of hydrogen density n_{H_2} for kinetic temperatures of 10 K, 20 K, 30 K and 40 K for transition $1_{10} - 1_{11}$ of H_2CS . Solid line is for $\gamma = 10^{-5} \text{ cm}^{-3} (\text{km/s})^{-1} \text{ pc}$ and the dotted line for $\gamma = 10^{-6} \text{ cm}^{-3} (\text{km/s})^{-1} \text{ pc}$. Keeping in view the accuracy of collisional rates available for some molecules, the factor of 2 is not very large. The collisional rate coefficients C_{14} and C_{23} used here are given in Table 4, as a function of temperature. In order to investigate sensitivity of our results to the collisional rates, we enhanced the collisional rates for the transitions with $\Delta k_a = 0$ by a factor of 10 which may be taken as an extreme case (Chandra & Shinde, 2004). The absorption feature of

the line is found to remain unaffected. However, the position of the minimum value of T_B is found to shift towards the low density region. With enhanced collisional rates the results for the brightness temperature T_B (K) are shown in column 4 of Figure 2.

Table 4. Collisional rate coefficients C_{14} and C_{23} in $\text{cm}^{-3} \text{s}^{-1}$ used in Figure 2

	$T_k = 10 \text{ K}$	20 K	30 K	40 K
C_{14}	1.370E-12	2.296E-12	2.976E-12	3.536E-12
C_{23}	2.796E-12	4.639E-12	5.993E-12	7.107E-12

(ii) When, we reduced the collisional rates for the transitions between the levels 1_{11} and 2_{11} by a factor of 2, the results given in Figure 3 show the brightness temperature T_B (K) (column 1), excitation temperature T_{ex} (K) (column 2) and the optical depth τ_ν (column 3) as a function of hydrogen density n_{H_2} for kinetic temperatures of 10 K, 20 K, 30 K and 40 K for transition $1_{10} - 1_{11}$ of H_2CS . Solid line is for $\gamma = 10^{-5} \text{ cm}^{-3} (\text{km/s})^{-1} \text{ pc}$ and the dotted line for $\gamma = 10^{-6} \text{ cm}^{-3} (\text{km/s})^{-1} \text{ pc}$. The collisional rate coefficients C_{14} and C_{23} used here are given in Table 5, as a function of temperature. In order to investigate sensitivity of our results to the collisional rates, here also we enhanced the collisional rates for the transitions with $\Delta k_a = 0$ by a factor of 10. The absorption feature of the line is found to remain unaffected. However, the position of the minimum value of T_B is found to shift towards the low density region. The results for the brightness temperature T_B (K) are shown in column 4 of Figure 3.

Table 5. Collisional rate coefficients C_{14} and C_{23} in $\text{cm}^{-3} \text{s}^{-1}$ used in Figure 3

	$T_k = 10 \text{ K}$	20 K	30 K	40 K
C_{14}	6.851E-13	1.148E-12	1.488E-12	1.768E-12
C_{23}	1.398E-12	2.320E-12	2.996E-12	3.553E-12

Figures 2 and 3 shows qualitatively that the transition $1_{11} - 1_{10}$ may show anomalous absorption. However, for the quantitative results, we have to go for the calculations for collisional rates.

7.1 Density dependence

Variation of brightness temperature T_B (K) with the molecular hydrogen density n_{H_2} shows that the maximum anomalous absorption occurs around a density of 10^4 cm^{-3} . For the higher densities, the brightness temperature T_B (K) increases and goes to a value higher than the background temperature (2.73 K) and then saturates to the value of the background temperature. In the low density region also the brightness temperature T_B (K) tends to the background temperature.

7.2 Temperature dependence

Figures 1 and 2 show that the maximum anomalous absorption is at the kinetic temperature of 10 K. The anomalous absorption decreases as the kinetic temperature in the cosmic object increases.

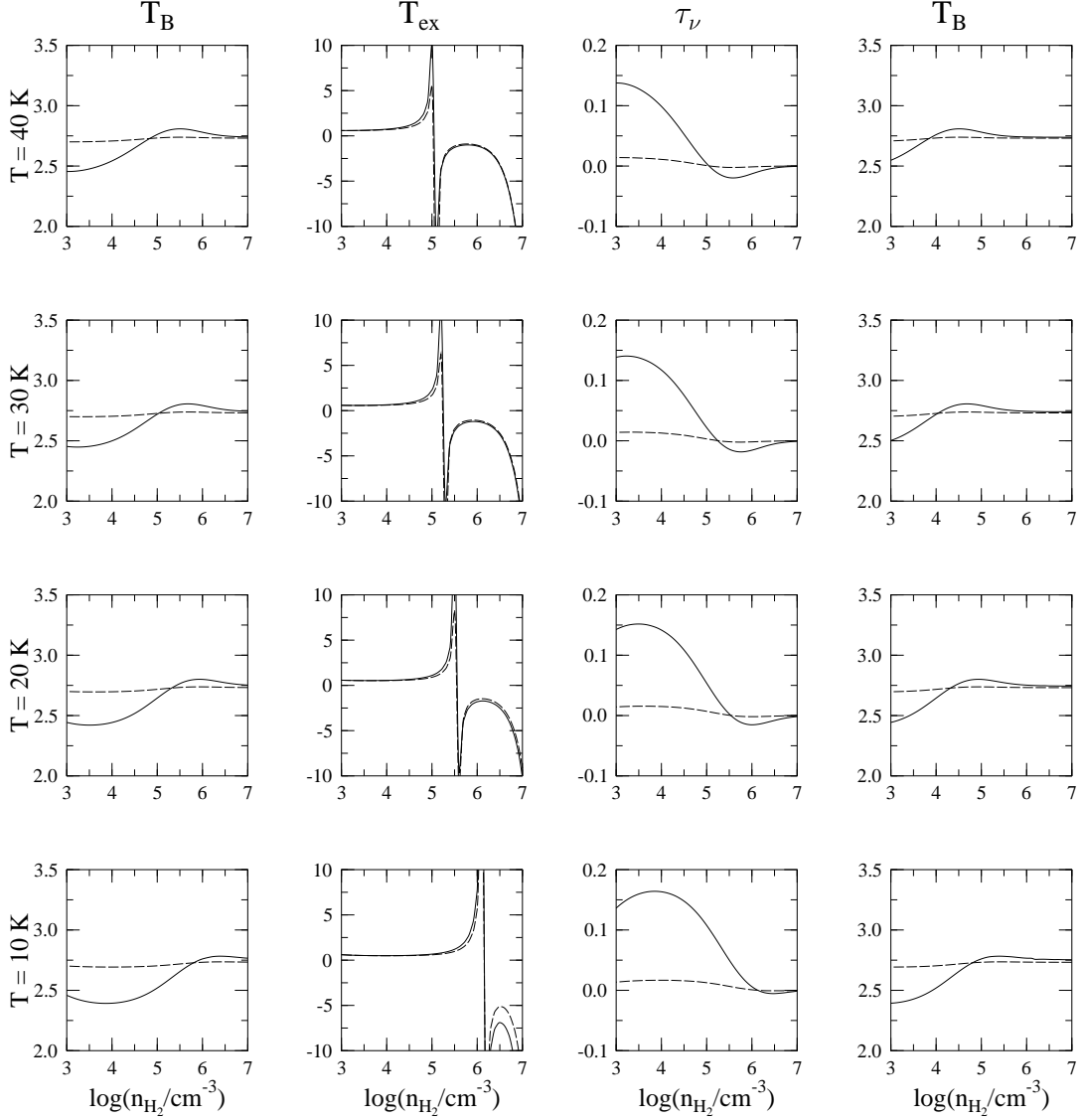


Figure 2: Variation of brightness temperature T_B (K) (column 1), excitation temperature T_{ex} (K) (column 2) and the optical depth τ_ν (column 3) versus hydrogen density n_{H_2} for kinetic temperatures of 10 K, 20 K, 30 K and 40 K for transition $1_{10} - 1_{11}$ at 1.0465 GHz of H_2CS . Solid line is for $\gamma = 10^{-5} \text{ cm}^{-3} (\text{km/s})^{-1} \text{ pc}$, and the dotted line for $\gamma = 10^{-6} \text{ cm}^{-3} (\text{km/s})^{-1} \text{ pc}$. For these results, the collisional rates between the levels 1_{10} and 2_{12} are increased by a factor of 2. The brightness temperature T_B (K) (column 4) is when the rates for the transitions with $\Delta k_a = 0$ are enhanced by a factor of 10.

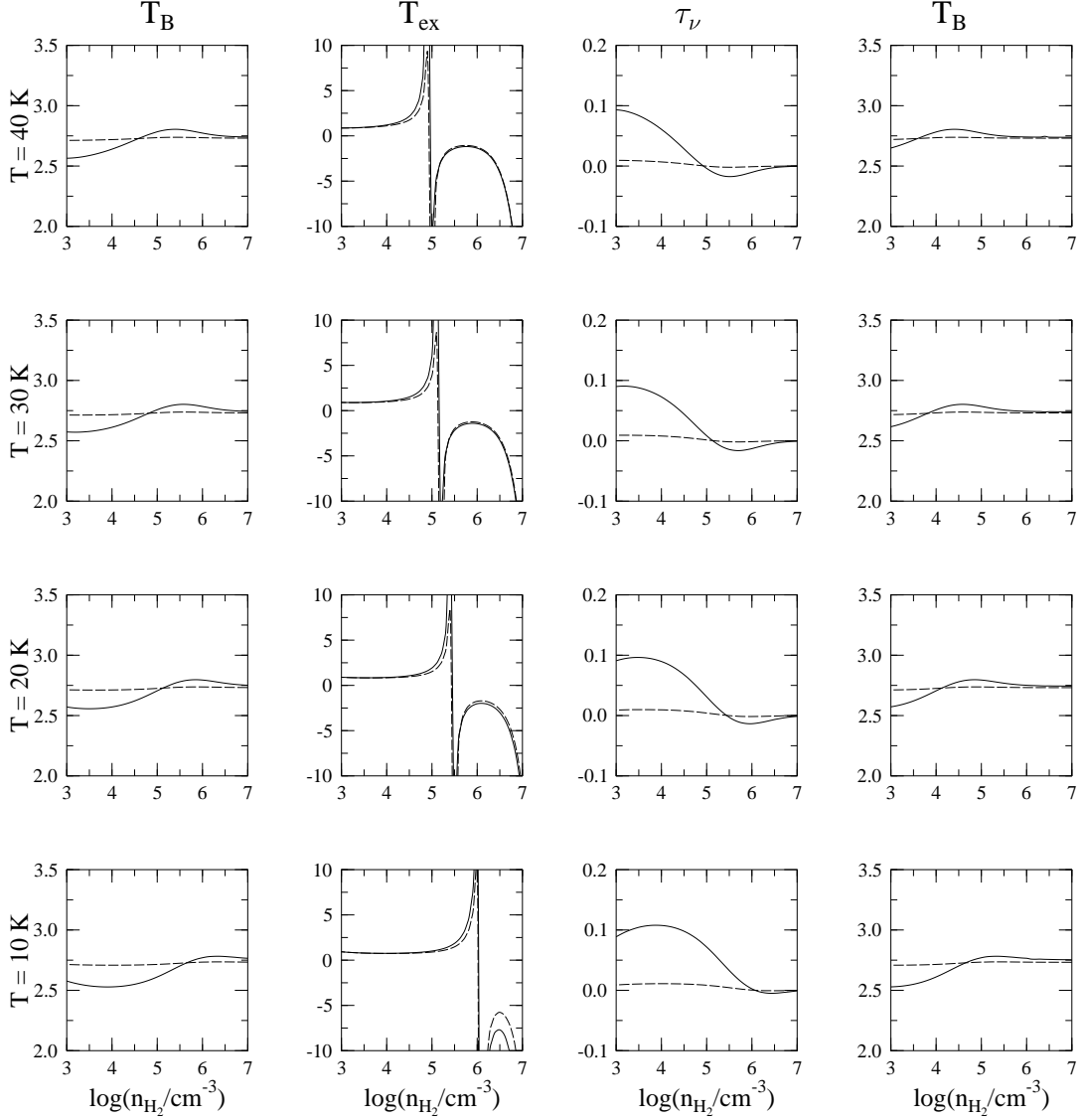


Figure 3: Variation of brightness temperature T_B (K) (column 1), excitation temperature T_{ex} (K) (column 2) and optical depth τ_ν (column 3) versus hydrogen density n_{H_2} for kinetic temperatures of 10 K, 20 K, 30 K and 40 K for transition $1_{10} - 1_{11}$ at 1.0465 GHz of H_2CS . Solid line is for $\gamma = 10^{-5} \text{ cm}^{-3} (\text{km/s})^{-1} \text{ pc}$, and the dotted line for $\gamma = 10^{-6} \text{ cm}^{-3} (\text{km/s})^{-1} \text{ pc}$. For these results, the collisional rates between the levels 1_{11} and 2_{11} are reduced by a factor of 2. The brightness temperature T_B (K) (column 4) is when the rates, for the transitions with $\Delta k_a = 0$ are enhanced by a factor of 10.

7.3 Comparison with H₂CO

In order to confirm our investigation, we did the calculations for H₂CO molecule where the molecular and distortional constants are taken from Bünken et al. (2003), given in column 3 of Table 1. Though the collisional rates for H₂CO are given by Green et al. (1978), but for H₂CO also we used the scaled values given by equation (1) and considered the similar variation for collisional rates. The collisional rate coefficients used in case of H₂CO are the same as given in Tables 4 and 5. The behaviour for the transition 1₁₁ – 1₁₀ for H₂CO was found similar to that of H₂CS. The anomalous absorption in H₂CO, by using the collisional rates of Green et al. (1978) has been investigated by Chandra et al. (2006b) and there also we found the similar behaviour.

8 Conclusions

Here, we have used scaled values of collisional rates for H₂CS, and therefore, our results are qualitative in nature. We found that the 1₁₁ – 1₁₀ may show anomalous absorption around the density of 10⁴ cm⁻³. This transition may help in identification of the molecule in cool cosmic objects, because the kinetic temperature may not be sufficient for generating the emission spectrum. But the anomalous absorption may be observed as the ground state is always populated. Since the value of $\mu^2 S(2I + 1)$ for the transition 1₁₀ – 1₁₁ is quite large, the transition 1₁₀ – 1₁₁ has large probability for its detection. Our future plan is to calculate collisional rates. Though the job is quite cumbersome and lengthy. Once the collisional rates are available, we can go for the quantitative results.

Acknowledgments

We are grateful to Prof. N.K. Bansal, Vice-Chancellor, SMVD University for encouragement. We are thankful to the anonymous referee for very constructive and appreciable comments, which helped us in the improvement of manuscript. Thanks are due to the DST, New Delhi and the ISRO, Bangalore for financial support in the form of research projects. A part of this work was done during the visit to the IUCAA, Pune. Financial support from the IUCAA, Pune is thankfully acknowledged.

References

- Beers, Y., Klein, G. P., Kirchhoff, W.H., Johnson, D.R., 1972. J. Mol. Spect. 44, 553.
- Brünken, S., Müller, H.S.P., Lewen, F., Winnewisser, G., 2003. Phys. Chem. Chem. Phys. 5, 1515.
- Chandra, S., Kegel, W. H., Varshalovich, D. A., 1984a. A&AS 58, 687.
- Chandra, S., Varshalovich, D. A., Kegel, W. H., 1984b. A&AS 55, 51.
- Chandra, S., Kegel, W.H., 2000. A&AS 142, 113.
- Chandra, S., Shinde, S.A., 2004. A&A 423, 325.
- Chandra, S., Musrif, P.G., Dharmkare, R.M., Sharma, M., 2006a. New Astronomy 11, 495.

- Chandra, S., Musrif, P.G., Shinde, S.V., 2006b. *Bull. Astr. Soc. India* 34, 11.
- Chandra, S., Shinde, S.V., Kegel, W.H., Sedlmayr, E., 2007. *A&A* 467, 371.
- Cox, P., Güsten, R., Henkel, C., 1987. *A&A* 181, L19.
- Davies, R.D., Booth, R.S., Pedlar, A., 1971. *Mon. Not. Roy. Astr. Soc.* 152, 7p.
- Evans, N.J., Townes, C.H., Weaver, H.F., Williams, D.R.W., 1970. *Science* 169, 680.
- Fabricant, B., Krieger, D., Muentner, J.S., 1977. *J. Chem. Phys.* 67, 1576.
- Forster, J.R., Goss, W.M., Wilson, T.L., Downes, D., Dickel, H.R., 1980. *A&A.* 84, L1.
- Green, S., Garrison, B.J., Lester Jr, W.A., Miller, W.H., 1978. *ApJS* 37, 321.
- Gordy, W., Cook, R.L., 1984. *Microwave Molecular Spectra* (New York: Wiley).
- Johnson, D.R., Powell, F. X., 1970. *Science* 169, 679.
- Johnson, D.R., Powell, F. X., Kirchhoff, W.H., 1971. *J. Mol. Spectrosc.* 39, 136.
- Madden, S.C., Irvine, W.M., Matthews, H.E., et al., 1989. *AJ* 97, 1403.
- Maeda, A., Medvedev, I.R., Winnemisser, M., De Lucia, F.C., Herbst, E., Müller, H.S.P., Koerber, M., Endres, C.P., Schlemmer, S., 2008. *ApJS* 176, 543.
- Marcelino, N., Cernicharo, J., Roueff, E., Gerin, M., Mauersberger, R., 2005. *ApJ* 620, 308.
- Palmer, P., Zuckerman, B., Bhul, D., Snyder, L.E., 1969. *ApJ* 156, L147.
- Schilke, P., Groesbeck, T.D., Blake, G.A., Phillips, T.G., 1997. *ApJS* 108, 301.
- Sinclair, M.W., Fourikis, N., Ribes, J.C., Robinson, B.J., Brown, R.D., Godfrey, P.D., 1973. *Austral. J. Phys.* 26, 85.
- Snyder, L.E., Bhul, D., Zuckerman, B., Palmer, P., 1969. *Phys. Rev. Lett.* 22, 679.
- Whiteoak, J.B., Gardner, F.F., 1983. *MNRS* 205, 27p.